

# From isolated porphyrin ligands to periodic Al-PMOF: A comparative study of the optical properties using DFT/TDDFT

Andrés Ortega-Guerrero, Maria Fumanal, Gloria Capano, and Berend Smit\*

*Laboratory of Molecular Simulation (LSMO), Institut des Sciences et Ingénierie Chimiques, Valais Ecole Polytechnique Fédérale de Lausanne (EPFL), Rue de l'Industrie 17, CH-1951 Sion, Switzerland*

E-mail: [E-mail:berend.smit@epfl.ch](mailto:berend.smit@epfl.ch)

## Abstract

The use of photosensitizers as organic ligands in Metal-Organic Frameworks (MOFs) is a common practice to improve their UV/Vis optical absorption. For instance, MOFs consisting of porphyrin ligands usually inherit their light-harvesting properties and thus follow the Gouterman model in which the low-lying excitations correspond to  $\pi \rightarrow \pi^*$  transitions. However, the characterization of the excited states of porphyrin ligands in MOFs requires an appropriate description of the periodic crystal including the metal nodes and inter-molecular interactions. Here, we investigate the UV/Vis absorption properties of the porphyrin-MOF Al-PMOF and two metallated forms, Zn-Al-PMOF and Co-Al-PMOF, and of their corresponding isolated porphyrin ligands using DFT/TDDFT simulations with PBE, PBE0, and CAM-B3LYP functionals. Our results indicate that hybrid functionals are necessary to capture the proper nature of the transitions and the excitonic effects of the optical and fundamental gaps in

porphyrin molecules and porphyrin-MOFs that PBE functional fails to describe. Likewise, the simulations show that a wrong representation of some excitations can be obtained depending on the functional and when the Tamm-Dancoff approximation is used. Finally, our results show that PBE and PBE0 functionals are not able to capture the gap-renormalization when going from the isolated molecules to the periodic crystals. Overall, the nature of the optical transitions, the excitonic effects, and the gap-renormalization are important features to assess in the prediction of optical properties in MOF crystals that require considering proper functionals and approximations to overcome the main failures of DFT/TDDFT calculations.

## Introduction

Metal-Organic frameworks (MOFs) have attracted significant attention as materials with the potential to be exploited in optical applications.<sup>1,2</sup> The modular inorganic-organic nature and the topology of their crystal structure make MOFs prospect materials for designing novel systems with unique photophysical and photochemical properties. In this regard, MOFs offer the advantage of tunability since their properties can be easily modified by the selection and/or modification of its constituent units.<sup>3</sup> The incorporation of photosensitizers as ligands in MOFs is of interest for improving the visible-light absorption profile. Such property can be beneficial in applications for light-harvesting and photocatalysis.<sup>4,5</sup> Inspired by the natural photosynthesis that occurs in highly ordered chlorophyll complexes, the incorporation of porphyrins in MOFs has been a recurrent strategy to exploit their optical properties.<sup>6-8</sup> This strategy has also been used in dye-sensitized solar cells, where the molecular engineered of porphyrin-based compounds improved the light-harvesting properties.<sup>9</sup>

Porphyrin MOFs have been synthesized using different transition metal nodes attempting to encompass the optical properties of porphyrin ligands within a porous framework.<sup>8,10</sup> Rosseinsky and coworkers synthesized a porphyrin MOF with Al(III) at the metal nodes named Al-PMOF (Figure 1a) which was found to be water-stable.<sup>11</sup> This material presents

visible-light-driven hydrogen generation when combined with ethylenediaminetetracetic acid and Pt nanoparticles. Porphyrins can easily coordinate metal ions, yielding to metallated-porphyrins that can boost the catalytic activity. With this purpose, Al-PMOF has been also reported in different metallated forms such as Zn-Al-PMOF<sup>11</sup> and Co-Al-PMOF<sup>12,13</sup> aiming to modify the catalytic and photophysical properties of the material. In previous studies, the ground state electronic properties of Al-PMOF have been extensively analyzed indicating that the frontier orbitals of the material are dominated by the orbitals of the porphyrin ligands.<sup>14,15</sup> For that reason, even though Al-PMOF is composed of porphyrin ligands and Al nodes, the optical properties of this MOF have been mainly attributed to the porphyrin ligands<sup>11</sup> neglecting the interaction with the metal-nodes and between porphyrin ligands. In this context, the optical properties of porphyrin molecules have been widely studied in both computational and experimental studies but a detailed analysis of the excited states and optical absorption properties of porphyrin-MOF materials is still missing. Certainly, excited-state phenomena in MOFs are not restricted solely to the ligands, where the interaction with the metal nodes can also lead to low-lying charge-transfer excited states.<sup>7,16</sup> Moreover, the crystal embedding may have a strong effect on the ligands properties and thus, it is necessary to apply computational approximations that are capable to describe this effect in periodic MOFs. The optimum design of MOFs with desired optical properties requires ultimately the understanding and prediction of their excited states, which in conjunction with other theoretical descriptors will define the final photophysical and photochemical properties of the material.<sup>17,18</sup> For this reason, an accurate description of their electronic and optical properties is needed.

Both the fundamental and the optical gap are of special interest in studying the optical properties of MOFs. The fundamental gap,  $E_{\text{fund}}$ , is the difference between the first ionization potential and the first electron affinity in both molecules and solids.<sup>19,20</sup> The position of these energy levels is of great importance for photocatalytic applications as they determine the capabilities of the system to promote a given reaction upon excitation.<sup>18</sup> The second gap is

the optical gap,  $E_{\text{opt}}$ , which is defined as the difference between the energies of the lowest dipole-allowed excited state and the ground state.<sup>19</sup> The optical band gap can be determined experimentally as the onset of the UV/Vis spectrum. Both band gaps can be in principle predicted by Density Functional Theory (DFT). In the case of a molecule, the  $E_{\text{fund}}$  can be directly obtained as the difference between the eigenvalues of the highest occupied molecular orbital (HOMO) and the lowest unoccupied molecular orbital (LUMO) energies. For the case of solids, it is the difference between the highest occupied crystal orbital (HOCO) and the lowest unoccupied crystal orbital (LUCO) energies. The frontier crystal orbital energies should be obtained from the highest and lowest energies in the band structure of the material, respectively. However, these can be directly computed at the  $\Gamma$ -point in the Brillouin Zone if these are located in this point.<sup>20</sup> Unfortunately, the previous statements only holds for the exact exchange-correlation(XC) functional, while in practice we can only use approximations for this functional.<sup>21</sup> It is noteworthy to mention that GGA functionals cannot provide the correct fundamental gap and global hybrid functionals usually also lead to an underestimated frontier orbital energy gap (especially in organic molecules).<sup>21</sup> The optical gap can be predicted using the eigenvalues obtained from DFT by its linear-response time-dependent DFT (TDDFT) extension. Within TDDFT it is possible to derive the excitation energies of the system as the poles the response function. The optical gap is then considered as the first dipole-allowed excitation energy obtained by TDDFT.<sup>19,21-23</sup> The solution of the linear-response can be done by solving the Casida equations including forward and backward transitions<sup>24</sup> or by the Tamm-Dancoff approximation (TDA)<sup>25</sup> that discards the backward transitions. The TDA has the advantage of being computationally simpler and has been shown to ameliorate some drawbacks of conventional TDDFT such as the triplet instability problem.<sup>26</sup> As in the case of the fundamental gap, the optical gap prediction is also susceptible to the approximations used to solve the exchange-correlation functional.

In this work, we perform a comprehensive study of the optical properties of the isolated porphyrin ligand and the porphyrin-MOF crystal of Al-PMOF by DFT and TDDFT com-

putations. We aim to evaluate the effect of the crystal embedding of the porphyrin ligands in MOFs. To do so, we study the performance of different DFT/TDDFT approximations in both isolated porphyrin ligands and periodic porphyrin-MOFs. We consider the isolated porphyrin ligand meso-Tetra(4-carboxyphenyl)porphine (TCPP) and the Zn(II) and Co(II) metallated forms (Figure 1b) to assess the effect of metallation on the optical properties of porphyrin Al-PMOF. This choice allows us to compare two model cases TPCC and Zn(II)-TPCC of porphyrin with a closed-shell electronic configuration, with a challenging open-shell system, Co(II)-TPCC, characterized by a partially occupied d-shell. First, we analyze the isolated porphyrin ligands to determine the characteristic excited state features as predicted by different functionals and considering full TDDFT and TDA implementations. We then study the properties of Al-PMOF material and the two different metallated forms Zn-Al-PMOF and Co-Al-PMOF at the same level of theory than the isolated systems. Aiming to compare the isolated and periodic systems, we use a computational setup based on a basis set and functionals that can be used in both periodic MOFs and isolated molecules. Finally, we perform a comparative analysis of the results of the periodic systems and the isolated ligands and discuss the performance and limitations of DFT to address the optical properties of porphyrin-MOFs.

## Computational details

### Molecular systems

The three porphyrin molecules, meso-Tetra(4-carboxyphenyl)porphine  $H_2$ TCPP, Zn(II) meso-Tetra(4-carboxyphenyl)porphine ZnTCPP, and Co(II) meso-Tetra(4-carboxyphenyl)porphine CoTCPP, were optimized using DFT with PBE,<sup>27</sup> PBE0,<sup>28,29</sup> and CAM-B3LYP<sup>30</sup> implemented in Gaussian 16.<sup>31</sup> The 6-31G\* basis set<sup>32</sup> was used for H, C, N, and O, while the LANL2DZ basis set with pseudopotentials was employed for Zn and Co.<sup>33</sup> We restrict our analysis to double- $\zeta$  with polarization basis set in order to fairly compare the results with

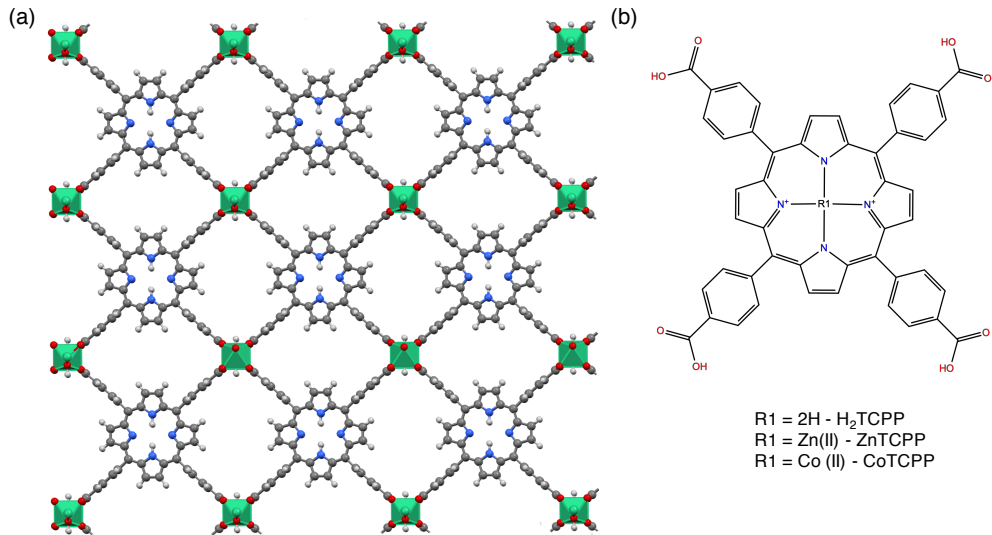


Figure 1: (a) Al-based porphyrin framework structure Al-PMOF. (b) meso-Tetra(4-carboxyphenyl)porphine H<sub>2</sub>TCPP, Zn(II) meso-Tetra(4-carboxyphenyl)porphine ZnTCPP and Co(II) meso-Tetra(4-carboxyphenyl)porphine CoTCPP.

the calculations in periodic calculations performed also with double- $\zeta$  polarization basis set. The optimization procedure was set to tight along with a super fine grid for the two-electron integrals. The optical absorption spectra were computed considering the full formulation of the Casida equations and the Tamm-Dancoff approximation using linear response TDDFT with the three different functionals.

## Periodic Systems

Starting from the known experimental single-crystal X-ray structure,<sup>11</sup> the periodic structures for the aluminium porphyrin MOF (Al-PMOF) and the ones with Zn (Zn-Al-PMOF) and Co (Co-Al-PMOF) were fully optimized using DFT implemented in the CP2K code.<sup>34,35</sup> The structures were optimized using the PBE XC functional with the D3 dispersion correction.<sup>36</sup> The electronic and optical properties of the MOFs were also studied with PBE0 functional.<sup>37</sup> The PBE calculations are conducted using a 1 x 2 x 1 supercell. For Co-Al-PMOF, we used an anti-ferromagnetic singlet orientation of the spin and the DFT+U scheme, where a Hubbard effective potential is added to the d orbitals of the Co atoms. The

Löwdin population analysis method<sup>38</sup> was used along with a Hubbard correction  $U_{\text{eff}}$  value of 3.5 eV. This U-value corrects the nature of the crystal orbitals in Co-Al-PMOF to the same symmetry of the ones obtained with PBE0. In addition, we also fully optimized the H<sub>2</sub>TCPP, ZnTCPP, and CoTCPP isolated molecules in CP2K to properly compare the fundamental and optical gap values obtained for the periodic MOF counterparts. In this case, the DFT+U method was used to compute its electronic ground state of CoTCPP. Calculations with CP2K used the QUICKSTEP program and mixed Gaussian and plane wave basis sets in combination with Goedecker-Teter -Hutter (GTH) pseudopotentials.<sup>39</sup> The efficient orbital transformation (OT) method<sup>40</sup> was used for the optimization of the wave function. The double- $\zeta$  polarization MOLOPT basis sets were used to describe H, O and N atoms, while a triple- $\zeta$  was used for Zn, Al, and Co atoms. In addition, for the PBE0 calculations, the auxiliary MOLOPT-ADMM basis functions<sup>41</sup> were used: cFIT8 for Al, cFIT11 for Zn and Co, and pFIT3 for non-metal atoms. The Truncated Coulomb operator with a long-range correction was employed for the Hartree-Fock exchange of hybrid calculations. The truncation radius is half of the smallest edge of the unit cell, and the long-range part of the exchange is computed using the PBE exchange. A plane-wave energy cutoff of 600 Ry was used, and the calculations were done using the gamma point over the irreducible Brillouin zone. The density of states and the crystal orbitals were computed using the PBE0 XC functional along with D3 dispersion correction using 1 x 2 x 1 supercell structures. The UV/Vis absorption spectra of the MOFs was computed using the PBE functional for Al-PMOF and Zn-Al-PMOF while DFT+U was used for Co-Al-PMOF using the LR-TDDFT implementation of CP2K. The optical gaps of the three materials were computed as well with PBE0. When applying LR-TDDFT using PBE0 the long-range correction is excluded according to the CP2K implementation.

# Results and discussion

## Molecular systems

The study of optical absorption properties in MOF can be performed considering full periodic boundary conditions<sup>42,43</sup> or using a representative cluster model.<sup>44–46</sup> In the case of Al-PMOF that corresponds to the isolated porphyrin ligands. The excited states of porphyrin molecules can be explained by the Gouterman four-orbital model.<sup>47</sup> According to this model, the excitations are characterized by  $\pi \rightarrow \pi^*$  transitions from the HOMO, HOMO-1 to the LUMO, LUMO+1 orbitals. Figure 2 shows the frontier orbitals of H<sub>2</sub>TCCP localized in the porphyrin core of the molecule and have the same symmetry of the Gouterman model. Although, porphyrin is only the macrocycle of H<sub>2</sub>TCCP, the presence of the carboxyphenyl groups does not affect frontier orbitals from the porphyrin group. Porphyrins absorb strongly in the 400–450 nm range (Soret or B band) and weakly in the 500–700 nm region (Q band).<sup>48</sup>

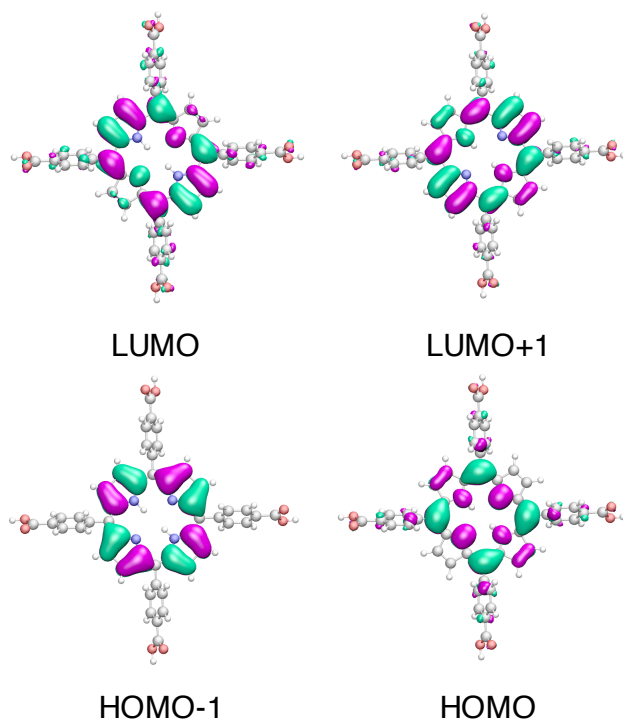


Figure 2: H<sub>2</sub>TCCP  $\pi$  and  $\pi^*$  frontier edge molecular orbitals involved in the Q and Soret bands transitions.



In general, the DFT packages available for periodic calculations implement LR-TDDFT solving the Casida equations within the Tamm-Dancoff approximation (TDA). In contrast, quantum chemistry software used for studying isolated molecular systems and cluster models implements both the full representation of the Casida equations and TDA. In order to determine the relevance of the TDA approach in the study of porphyrin ligands, we computed the UV/Vis spectra using both full TDDFT and TDA on the isolated molecules and compared them with the experimental results. In this way, we can fairly compare with the TDA absorption spectra of the periodic systems, which is shown in the next section.

Figure 3 shows the different spectra of H<sub>2</sub>TCPP, ZnTCPP, and CoTCPP molecules computed with TDDFT and TDA using PBE, PBE0, and CAM-B3LYP functional. In this figure, we also compare the compute spectra with the experimental ones. It is important to mention that the experimental Q bands in H<sub>2</sub>TCPP are four while in ZnTCPP are two. The difference comes from the metallation with the Zn ion which increases the symmetry from  $D_{2h}$  to  $D_{4h}$  point group in the porphyrin macrocycle.<sup>49,50</sup> This change in symmetry causes a degeneracy of the LUMO and LUMO+1 orbitals in ZnTCPP. For the case of H<sub>2</sub>TCPP, there are two separate Q band excitations that further split into four due to vibrational coupling while ZnTCPP should have two degenerate Q bands that split due to vibrational coupling. For the case of CoTCPP, the Q bands do not further split as much as ZnTCPP and are observed as one single Q band. In the absence of vibrational coupling, the Q bands appear as double and single peaks in the TDDFT calculations for H<sub>2</sub>TCPP and ZnTCPP, respectively.

To discuss the results, we should make a difference between H<sub>2</sub>TCPP and ZnTCPP, which are closed-shell systems, and CoTCPP which is an open-shell system with a partially occupied d-shell. For H<sub>2</sub>TCPP and ZnTCPP, the three XC functionals describe the frontier molecular orbitals as in the Gouterman-model (Figures S1 and S2) and only differ by their Kohn-Sham energy gap (Tables S1 and S3). The three functionals predict with good accuracy the position of the Q bands in comparison with the experimental spectra (Figure 3). The

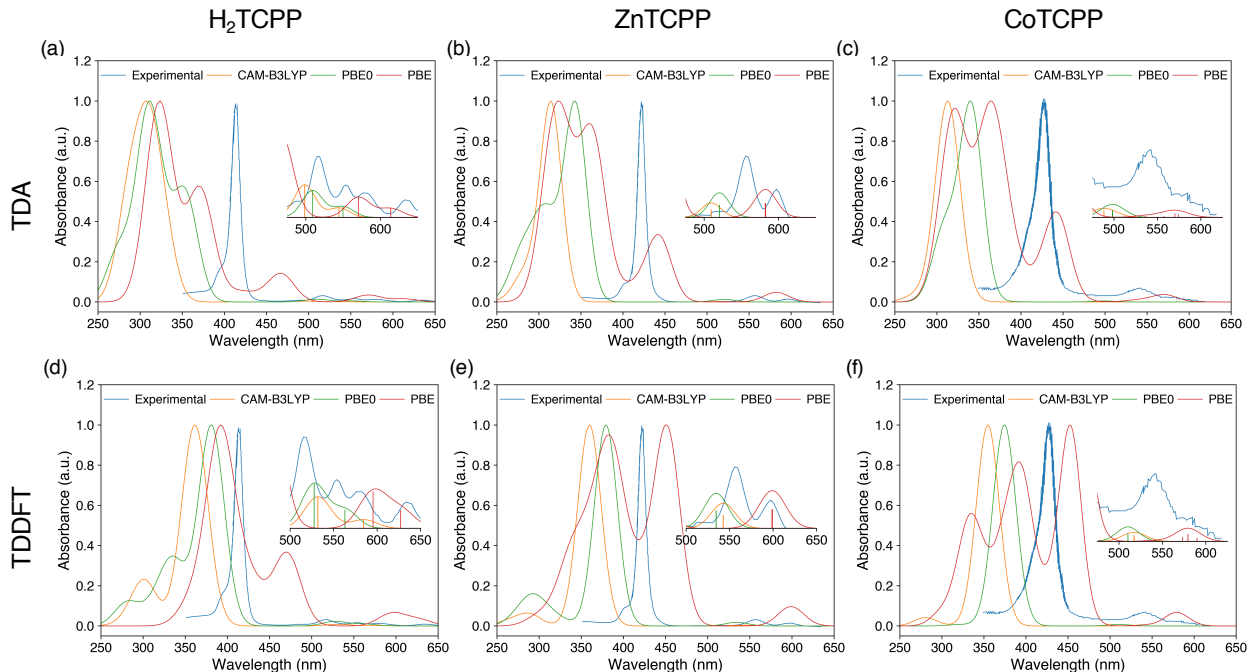


Figure 3: Comparison of the experimental UV/Vis absorption spectra and the TDDFT calculations using different XC functionals of the porphyrin molecules. The upper row considers the Tamm-Dancoff approximation while the lower row the full solution of the Casida equations for (a) and (d)  $\text{H}_2\text{TCPP}$ , (b) and (e)  $\text{ZnTCPP}$ , (c) and (f)  $\text{CoTCPP}$  respectively. The theoretical UV/Vis spectra are normalized. Experimental spectra of  $\text{H}_2\text{TCPP}$  and  $\text{ZnTCPP}$  are taken from ref.<sup>51</sup> and  $\text{CoTCPP}$  are taken from ref.<sup>52</sup> Insets: enlarged spectra of the Q bands.

use of TDA or the full Casida formalism have a small impact on the positioning of the Q bands. In particular, the Q bands when evaluated with the TDA are slightly blue-shifted with respect to their position when using the full Casida formalism, regardless of the XC functional used. Similarly, the use of a pure hybrid XC PBE0 and a range-separated XC CAM-B3LYP results in the Q bands only slightly blue-shifted with respect to the PBE results. Thus, the performance of PBE on the prediction of the optical gap (Q Bands) in porphyrin molecules is rather good, as has been previously reported.<sup>19</sup> Although PBE predicts the optical gap with good accuracy, the value obtained is larger than the PBE fundamental gap, which indicates a misrepresentation of the excitonic effects.<sup>19,22</sup> Given the local excitation nature of the Q bands ( $\pi \rightarrow \pi^*$ ), this will imply a repulsive interaction between the electron and hole. This artifact is preserved in all the PBE calculations with TDA and full TDDFT

(Tables S1, S2, S3 and S4). The use of hybrid or range-separated XC functionals corrects this artifact resulting in larger fundamental gap predictions and therefore, attractive excitonic effects (Tables S1 and S3). Another feature observed in the PBE spectra is the presence of additional excitations between the Soret band and Q bands. According to the Gouterman model, the Soret excitations should be predicted right after the Q bands. However, H<sub>2</sub>TCPP and ZnTCPP UV/Vis spectra using PBE predict additional absorption peaks providing a wrong description of the experimental spectrum. These additional peaks appear as a result of a strong underestimation of charge-transfer (CT) states within TDDFT<sup>53</sup> evaluated with a pure GGA functional. These excitations correspond to CT transition from the porphyrin macrocycle to the phenyl orbitals of the molecule, which is observed in both TDA and full-Casida formalism calculations. Due to the artificial underestimation of the CT states within PBE, the Soret band shows a mixture of orbital contributions and thus has been analyzed using Natural transition orbitals (NTO) to assign the peaks (Figures S9, S10, S14 and S14).

In contrast, PBE0 and CAM-B3LYP functionals show the proper description of the excitations of the porphyrin molecules within the UV/Vis range in good agreement with the experimental measurements. In both molecules, the Soret band appears as the third excitation in the full Casida TDDFT calculations (Table S1 and S3). When using TDA with PBE0 the previous statement only holds for ZnTCPP but not for H<sub>2</sub>TCPP. For the latter, additional excitations of CT character from the porphyrin to the phenyl groups appear below in energy (Figure S8). These additional excitations observed in H<sub>2</sub>TCPP with PBE0 and TDA remain when larger basis set are considered as well (Figure S17). Although PBE0 functional can still be susceptible to CT artifacts in TDDFT,<sup>53</sup> an over-stabilization of the CT states is only observed with TDA applied to the H<sub>2</sub>TCPP ligand. This error is not observed with CAM-B3LYP in any case. Altogether, the spectra predicted with the three XC functionals for H<sub>2</sub>TCPP and ZnTCPP showed the Soret band less blue-shifted with respect to the experiments when using the full-Casida TDDFT formalism instead of the TDA. Despite that the TDA has been found to very accurate when used to organic molecules,<sup>54</sup> our

calculations show a significant improvement of the porphyrin UV/Vis spectrum when using the full TDDFT approach. Yet, it is important to mention that the TDA does not fail in the description of the porphyrin excitations. The failure of TDA to fully recover the appropriate ordering and energetics of the CT and local states of porphyrin molecules suggests that important electronic correlation is missing when neglecting the backward contributions to the transitions.<sup>55</sup>

The description of the UV/Vis properties of CoTCPP is a bigger challenge for both DFT and TDDFT. In particular, the ground state properties must be computed by DFT using an unrestricted Kohn-Sham formalism.<sup>56</sup> Unrestricted DFT and TDDFT calculations for open-shell systems are susceptible to spin-contamination from having  $\alpha$  and  $\beta$  electrons treated independently. In addition, Co(II) has a partially occupied d-shell, whose electrons are highly correlated. These challenges lead to the necessity of using more accurate and computationally demanding functionals to ensure an appropriate description of the ground state and usually imply highly demanding TDDFT calculations including a large number of excitations.

First, we consider the description of the ground state properties of CoTCPP. The PBE calculations of CoTCPP suffer from a high self-interaction error and result in frontier molecular orbitals that do not follow the Gouterman model (Figure S3). This error mainly originates from the presence of an unpaired electron in the d-shell of the Cobalt atom and can be partially fixed by considering a hybrid functional. Indeed, the PBE0 and CAM-B3LYP functionals reduced the self-interaction error and predicted the frontier molecular orbitals of CoTCPP in agreement with the Gouterman model (Figure S4). Remarkably, the calculations performed with PBE also alter the molecular structure of CoTCPP, which shows a distorted non-planar shape of the porphyrin macrocycle in contrast to the planar structure obtained with PBE0 (Figure S5).

Second, we analyse the optical absorption properties of CoTCPP. Figures 3c and 3c show the TDDFT UV/Vis spectra compared with the experimental measurement using TDA and

the full-Casida formalism. Like in the case of H<sub>2</sub>TCPP and ZnTCPP, the UV/Vis spectra of CoTCPP computed with the hybrid and range-separated functionals show good agreement with the experimental spectra, being the TDA spectra slightly blue-shifted with respect to the full-Casida approach in all cases. On the other hand, the PBE calculations predict that the lowest excitations correspond to d-d transition (with an almost zero oscillator strength) instead of the Q bands (Tables S5 and S6). However, the Q bands appear after this d-d excitations and have a higher oscillator strength as shown in the UV/Vis spectra (Figures 3c). Although PBE fails to properly describe the ground properties of CoTCPP, it predicts the Q bands in agreement with the Gouterman-model and with the experimental wavelength, while still suffers from the same problems encountered in H<sub>2</sub>TCPP and ZnTCPP showing additional excitations between the Q bands and Soret Band. Moreover, the PBE results shows large spin contamination in the low lying transitions up to values of  $S^2$  of 1.5 (being ideally 0.75) (Table S5 and S6).

The TDDFT calculations using hybrid and range-separated functionals entail a larger computational cost for CoTCPP than for H<sub>2</sub>TCPP and ZnTCPP. As previously mentioned, the use of unrestricted TDDFT in conjunction with a partially occupied d-shell requires to include a higher number of excitations than in the restricted TDDFT case with either a purely organic or fully occupied d-shell system. The first 10 excitations in CoTCPP computed with PBE0 and CAM-B3LYP functionals are all dark excitation (oscillator strength equals to zero), mostly including low energy d-d local excitations. Excitations  $S_{11}$  and  $S_{12}$  correspond to the Q bands of the porphyrin and thus properly represent the optical gap with negligible spin contamination (Table S5 and S6). As in the case of H<sub>2</sub>TCPP and ZnTCPP, the NTO analysis of the full-Casida TDDFT calculations shows that both PBE0 and CAM-B3LYP functionals describe properly the Soret bands in CoTCPP. However, the NTO analysis of the TDA results obtained with CAM-B3LYP shows that the some d orbitals of Co(II) are involved in one of the Soret bands transition (Figure S15) thus misrepresenting the character of this excitation. Overall our results suggest that the full Casida formulation

should be considered when studying the optical UV/Vis excitations of porphyrin ligands instead of TDA. According to our calculations, we encounter some additional excitations ( $\text{H}_2\text{T CPP}$ ) and the wrong description of the orbitals of the Soret band ( $\text{CoT CPP}$ ) when using this approximation. It is noteworthy to mention that the last statement only holds for the basis set we consider here. Despite that GGA functionals are able to properly predict the Q bands of porphyrin ligands, these functionals have important issues to correctly account for the excitonic effects in the  $E_{\text{opt}}$  and may over-stabilize charge-transfer states between the porphyrin and its substituent units in the UV/Vis spectrum.

## Periodic Systems

MOFs systems containing porphyrins have the additional challenge of addressing the optical properties in periodic boundary conditions plus the presence of the transition metal nodes. Herein, we considered Al-PMOF built from Aluminium metal nodes connected to porphyrin ligands in a 3D network (Figure 1a). The optimization in periodic boundary conditions of Al-PMOF using PBE functional with D3 dispersion correction shows good agreement with the unit cell parameters published experimentally.<sup>11,57</sup> Figure 4 shows the projected density of states of Al-PMOF, as well as the systems where the porphyrin is metallated with Zinc (Zn-Al-PMOF) and Cobalt (Co-Al-PMOF) at the PBE0 theory level. The band gaps are 2.81, 2.93 and 3.12 eV for Al-PMOF, Zn-Al-PMOF and Co-Al-PMOF, respectively. The valence and conduction bands of the three MOFs are mainly dominated by orbitals localized on the porphyrin ligands. The band edge orbitals have the same symmetry ( $\pi$  and  $\pi^*$ ) as the ones of the isolated molecules (Figure S18 and S19). Likewise, these orbitals are highly localized presenting minimal dispersion.<sup>57,58</sup> The orbitals above the conduction band are higher energy orbitals from the porphyrin and also orbitals localized in the phenyl groups including the carboxylic groups. The electronic properties of Al-PMOF, Zn-Al-PMOF, and Co-Al-PMOF depicts a material where its electronic and optical properties are highly dominated by the porphyrin ligands.<sup>57</sup> There are not major changes in the electronic properties of the material

after changing the metal center of the porphyrin molecule (Figure 4).

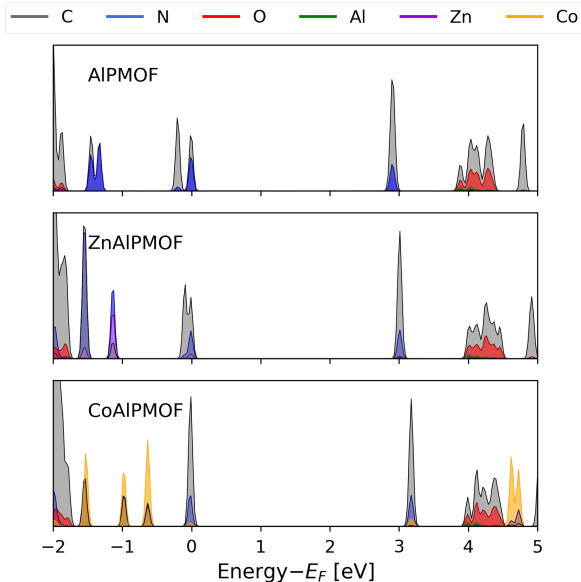


Figure 4: Projected density of states of Al-PMOF, Zn-Al-PMOF, and Co-Al-PMOF using PBE0 XC functional.

Calculations performed for Al-PMOF and Zn-Al-PMOF with PBE0 result in same band edge orbitals than the ones obtained with PBE considering the opening of the band gap in the hybrid calculations (Figure S22). However, in the case of Co-Al-PMOF, the description of the frontier orbitals remains challenging using PBE due to important self-interaction error effects.<sup>59</sup> As previously mentioned, these arise from the presence of Co(II) with an unpaired electron in the porphyrin ligand. In particular, the use of GGA functionals leads to a misrepresentation of the LUMO, which is the  $d_{z^2}$  orbital of the Cobalt ion instead of the  $\pi^*$  orbital of the porphyrin (Figure S20) as observed for the isolate CoTCPP molecule. Likewise, the use of a hybrid functional corrects the description of frontier orbitals of CoTCPP in Co-Al-PMOF, placing the  $d_{z^2}$  orbital of the Cobalt ion at higher energies (Figure S4). Interestingly, the CoTCPP ligand in Co-Al-PMOF does not display a non-planar shape when optimized with PBE (S5). Instead, the presence of the Aluminium backbone and the confined environment promotes a more planar structure in agreement with the experimental structure.

Taking into account our analysis on the use of PBE and PBE0 XC functionals to describe the electronic and structural properties of porphyrin-MOF, in the following we are going to focus on the study of their optical absorption properties. Since Co-Al-PMOF ground state is misrepresented with PBE, we use DFT+U calculations to correct the energy and character of its frontier crystal orbitals. A Hubbard  $U_{\text{eff}} = 3.5$  eV corrects the crystal orbitals in Co-Al-PMOF resulting in symmetries similar to the ones obtained with PBE0 (Figure S23 and S21). The DOS obtained with DFT+U display the correct band edges of the material as the ones obtained from PBE0 being slightly less localized (Figure S21). Figure 5 shows the comparison between the TDDFT with TDA computed spectra and the experimental UV/Vis spectra of Al-PMOF, Zn-Al-PMOF, and Co-Al-PMOF. We used PBE for Al-PMOF and ZnAlMOF while DFT+U method was used for Co-Al-PMOF. The periodic TDDFT with TDA calculations predict the Q bands in agreement with the experimental measurements. These Q bands have a 100% contribution from the band edge orbitals following the Gouterman four-orbital model. Additional excitations between the Soret and Q bands were also observed, as in the case of the isolated molecules. These additional excitations between the Soret and Q band do not correspond to transitions between the band edges orbitals exclusively. Instead, these transitions involve orbitals also from the phenyl group being of the same nature as the ones observed for the isolated molecules using PBE functional. Likewise, the highest absorption peak obtained for the periodic MOFs is not entirely described by the Gouterman four-orbital of the Soret band, instead it shows less than a 50% contribution of the  $\pi$  and  $\pi^*$  orbitals. The UV/Vis calculations spectra of the three MOFs are qualitatively similar to the experimental measurements. Yet, there are many additional transitions wrongly describing the character of the excitations in the entire UV/Vis spectra. PBE is the most common functional for the calculation of the UV/Vis spectra of periodic MOFs<sup>43,60</sup> since its computational cost allows to obtain the necessary number of excitations to cover the UV/Vis range. Based on our results, this functional has important difficulties to describe the upper region of the UV/Vis spectra in porphyrin MOFs, while predicts properly the Q



bands of Al-PMOF and its metallated counterparts.

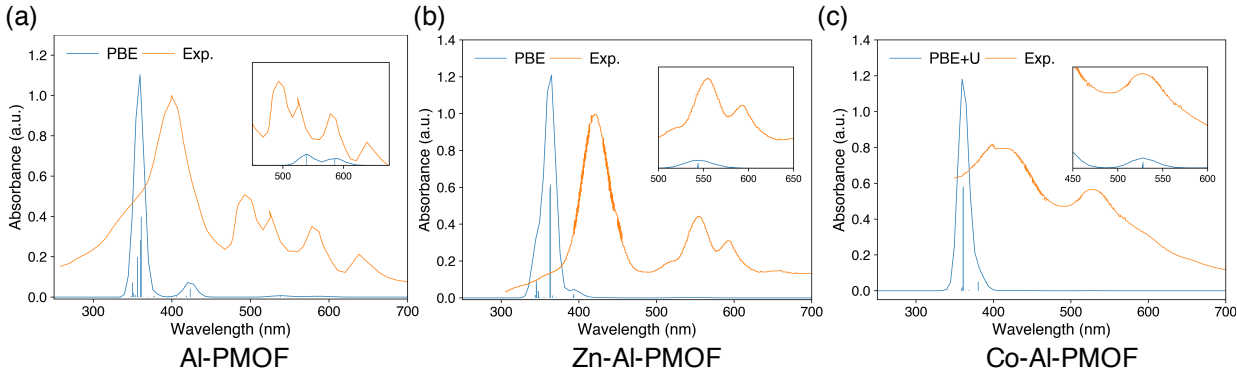


Figure 5: Comparison of the experimental UV/Vis absorption spectra and the periodic TDDFT calculations using a  $1 \times 2 \times 1$  supercell of (a) Al-PMOF and (b) Zn-Al-PMOF using the PBE XC functional, and (c) Co-Al-PMOF using the PBE+U XC functional with  $U_{\text{eff}} = 3.5$  eV. Al-PMOF and Zn-Al-PMOF UV/Vis spectra is taken from ref.<sup>11</sup> while Co-Al-PMOF is taken from ref.<sup>13</sup> Insets: enlarged spectra of the Q bands.

## Molecular vs periodic systems

Table 1: Comparison of the Fundamental Gap ( $E_{\text{fund}}$ ) and Optical gap ( $E_{\text{opt}}$ ) of the MOFs and isolated ligands using PBE and PBE0 calculations.

System	PBE		PBE0	
	$E_{\text{fund}}$ [eV]	$E_{\text{opt}}$ [eV]	$E_{\text{fund}}$ [eV]	$E_{\text{opt}}$ [eV]
Al-PMOF	1.820	2.110	2.879	1.801
Zn-Al-PMOF	1.960	2.140	2.993	1.930
Co-Al-PMOF*	2.082	2.348	3.161	1.898
H <sub>2</sub> TCPP	1.798	2.068	2.929	1.861
ZnTCPP	1.893	2.197	3.037	1.975
CoTCPP*	2.049	2.290	3.202	2.099

\* The PBE results are from PBE+U calculations.

According to the calculations of the isolated porphyrin molecules, a proper description of the UV/Vis spectra in porphyrin-MOFs requires a hybrid functional. However, computing the necessary number of excitations to cover the full range of the UV/Vis spectra using a hybrid functional is computationally too demanding. Instead, we computed the necessary

excitations in the lower energy range to evaluate the Q bands energies in the three porphyrin-MOF materials using PBE0, which correspond to excitations localized in the porphyrin macrocycle. We have computed the  $E_{\text{opt}}$  from TDDFT with TDA calculation as the first dipole allowed excitation. Table 1 shows a comparison of  $E_{\text{fund}}$  and  $E_{\text{opt}}$  computed with PBE and PBE0 XC functionals in the periodic MOFs and the isolated porphyrin ligands, except for Co-Al-PMOF and CoTCPP for which DFT+U was used instead of PBE. The values of  $E_{\text{fund}}$  and  $E_{\text{opt}}$  of the isolated porphyrin molecules shown in Table 1 were recomputed with CP2K to properly compare with the periodic calculations. It can be seen that the use of hybrid functionals increases the  $E_{\text{fund}}$  from the underestimated values obtained with PBE. Moreover, the  $E_{\text{fund}}$  have a similar value when computed in the periodic MOF and the associated isolated ligands, when using both PBE and PBE0 functionals. The results shows no major differences from computing  $E_{\text{fund}}$  for the isolated porphyrin molecule or from the periodic MOF. Considering that the frontier crystal orbital of the porphyrin-MOFs are of the same nature as in the Gouterman-model in isolated porphyrin molecules, that implies that neither PBE and PBE0 functionals are able to capture the gap re-normalization of going from an isolated molecule to a periodic crystal.<sup>19,21,23,61</sup> This re-normalization implies that the fundamental gap of an isolated molecule should be wider than the one of the same molecule as part of a periodic crystal. Although the last statement generally applies strongly to organic crystals, MOFs can inherit similar behavior given the limited electronic coupling and localized nature of their orbitals. In the case of the  $E_{\text{opt}}$ , the calculations using PBE on the periodic MOFs show the same behavior of their isolated ligand counterparts resulting in higher  $E_{\text{opt}}$  than the ones of their obtained for  $E_{\text{fund}}$ . This artifact from DFT/TDDFT using GGA functionals in porphyrins is reduced when a hybrid functional is used.<sup>22</sup> The PBE0 calculations show large  $E_{\text{fund}}$  than reduced  $E_{\text{opt}}$  depicting properly the excitonic effect nature of the Q Bands of both periodic MOFS and isolated ligands. The values of  $E_{\text{opt}}$  from PBE0 calculation are smaller than the PBE ones like it is observed in the isolated molecule calculations. Overall, Table 1 shows no significant differences in the  $E_{\text{fund}}$  and  $E_{\text{opt}}$

between calculations of the isolated molecules or the periodic MOFs. This last observation is in agreement with the nature of the electronic and optical properties of Al-PMOF being directed dominated by the porphyrin ligands.

Excitonic effects and gap-renormalization represent major challenges for the accurate prediction of the electronic and optical properties of MOFs. In general, experimental measurements of band gaps in MOFs are limited to the optical band gaps.<sup>62</sup> Usually, DFT calculations conducted in MOFs use the Kohn-Sham values to be compared with the reported values of experimental measurements of the optical gap, and this comparison is in principle incorrect. We said in principle, since in experimental conditions there are more effects to consider, as thermal effects and the quantum motion of the nuclei affecting both  $E_{\text{fund}}$  and  $E_{\text{opt}}$ .<sup>43,63</sup> In the field of bulk inorganic semiconductors, such comparison can hold given that excitonic effects are usually small, making the energy difference between  $E_{\text{fund}}$  and  $E_{\text{opt}}$  negligible. The strategy to overcome such challenges (gap-renormalization and excitonic effects) in organic crystals is to include the effect of the dielectric response along with optimally-tuned range-separated functionals by enforcing the Koopmans' condition.<sup>23,61</sup> In the case of MOFs, these calculations can be computationally demanding given the number of atoms and size of the unit cell. However such calculations are required to properly described their electronic and optical properties of MOFs. Here, we use a truncated and long-corrected PBE0 functional that, despite not being optimized, is capable to describe the excitonic effects in Al-PMOF and its metallated forms due to the strong localization of the frontier crystal orbitals in the porphyrin ligands.

## Conclusions

In this work, we have performed DFT and TDDFT calculations of Al-PMOF, Zn-Al-PMOF, and Co-Al-PMOF to asses the performance of different computational approximations to predict their electronic and optical absorption properties. To do so, we have first considered

the isolated porphyrin ligands of the three periodic MOFs and analyzed their ground state and excited state properties as obtained with PBE, PBE0 and CAM-B3LYP functionals. Our calculations reveal that different artifacts are obtained with the PBE functional. First, additional absorption bands are shown between the Soret and Q bands in the UV/Vis spectrum ascribed to charge transfer transitions from the porphyrin to its phenyl substituent. Second, the computed optical gap is larger than the fundamental gap thus resulting in a wrong representation of the excitonic effects. For that reason, we conclude that to study UV/Vis spectra in porphyrins and to correctly describe their optical excitations at least a hybrid functional is required. Evaluation of the optical spectra with the full-Casida formalism or TDA shows that TDA tends to predict a blue-shifted spectra and in some cases, additional excitations ( $\text{H}_2\text{TCCP}$ ) and the wrong description of the orbitals of the Soret band ( $\text{CoTCCP}$ ) are obtained. According to our calculations, the full-formalism shows better agreement with the experimental UV/Vis measurements and predicts the correct ordering and character of the states. This discrepancies between full TDDFT and TDA suggest that the electronic correlation of the backward excitations is important for the simulation of optical properties in porphyrins. The same conclusions apply for periodic porphyrin-MOFs. Our results show that the optical properties of Al-PMOF and its two metallated forms, Zn-Al-PMOF and Co-Al-PMOF, follow the Gouterman four-orbital model<sup>47</sup> in which the lowest excitations are characterized by  $\pi \rightarrow \pi^*$  transitions between the frontier crystal orbitals localized in the porphyrin ligands. Remarkably, both PBE and PBE0 functionals lead to an accurate prediction of the optical gap. However, both fail to capture the gap re-normalization of going from an isolated molecule to a periodic crystal.

It is important to note that the above results can be translated to other MOFs. The presence of localized orbitals from the organic ligands at the band structure edges of the MOF is a common feature, which is obtained when the orbitals of the metal-nodes are too high in energy with respect to the orbitals of the ligand. In such case, the ligand strongly influences the optical properties of the material. Thus, the performance of the DFT/TDDFT

approximations observed to describe the isolated ligands is translated to the periodic MOF. This may include a wrong representation of the excitonic effects and the character of the lowest excited states. The presence of additional ligands and transition metals with low-lying energy levels represent a major challenge for TDDFT when charge-transfer states are accessible. Additionally, calculations performed for periodic MOFs and isolated ligands may suffer from a wrong gap-renormalization description when using traditional functionals available for solids such as PBE and PBE0.

## Acknowledgement

This work has been supported by the Swiss National Science Foundation (SNSF) under Grant 200021\_172759 and the National Centre of Competence in Research (NCCR) Materials Revolution: Computational Design and Discovery of Novel Materials (MARVEL), and the European Research Council (ERC) under the European Union’s Horizon 2020 research and innovation programme (grant agreement 666983, MaGic). The authors also acknowledge PRACE for awarding the computing time on the GCS Supercomputer SuperMUC at Leibniz Supercomputing Centre ([www.lrz.de](http://www.lrz.de)). Calculations were performed as well at the EPFL High Performance Computer Center SCITAS and at the Swiss National Supercomputing Centre (CSCS) under project ID s1005.

## Supporting Information Available

Isolated molecules Orbitals and TDDFT results using TDA or full-Casida approach, Natural transition orbital analysis, Periodic MOFs crystal orbitals and DOS comparison using different functionals.

## References

- (1) Xiao, J.-D.; Jiang, H.-L. Metal–Organic Frameworks for Photocatalysis and Photothermal Catalysis. *Accounts of Chemical Research* **2019**, *52*, 356–366.
- (2) Cui, Y.; Zhang, J.; He, H.; Qian, G. Photonic functional metal–organic frameworks. *Chem. Soc. Rev.* **2018**, *47*, 5740–5785.
- (3) Nidamanuri, N.; Saha, S. *Functional Supramolecular Materials: From Surfaces to MOFs*; The Royal Society of Chemistry, 2017; pp 217–246.
- (4) So, M. C.; Wiederrecht, G. P.; Mondloch, J. E.; Hupp, J. T.; Farha, O. K. Metal–organic framework materials for light-harvesting and energy transfer. *Chem. Commun.* **2015**, *51*, 3501–3510.
- (5) Feng, X.; Pi, Y.; Song, Y.; Brzezinski, C.; Xu, Z.; Li, Z.; Lin, W. Metal–Organic Frameworks Significantly Enhance Photocatalytic Hydrogen Evolution and CO<sub>2</sub> Reduction with Earth-Abundant Copper Photosensitizers. *Journal of the American Chemical Society* **2020**, *142*, 690–695, PMID: 31895984.
- (6) Son, H.-J.; Jin, S.; Patwardhan, S.; Wezenberg, S. J.; Jeong, N. C.; So, M.; Wilmer, C. E.; Sarjeant, A. A.; Schatz, G. C.; Snurr, R. Q.; Farha, O. K.; Wiederrecht, G. P.; Hupp, J. T. Light-Harvesting and Ultrafast Energy Migration in Porphyrin-Based Metal–Organic Frameworks. *Journal of the American Chemical Society* **2013**, *135*, 862–869, PMID: 23249338.
- (7) Lan, G.; Zhu, Y.-Y.; Veroneau, S. S.; Xu, Z.; Micheroni, D.; Lin, W. Electron Injection from Photoexcited Metal–Organic Framework Ligands to Ru<sub>2</sub> Secondary Building Units for Visible-Light-Driven Hydrogen Evolution. *Journal of the American Chemical Society* **2018**, *140*, 5326–5329, PMID: 29578703.

- (8) Feng, L.; Wang, K.-Y.; Joseph, E.; Zhou, H.-C. Catalytic Porphyrin Framework Compounds. *Trends in Chemistry* **2020**,
- (9) Mathew, S.; Yella, A.; Gao, P.; Humphry-Baker, R.; Curchod, B. F. E.; Ashari-Astani, N.; Tavernelli, I.; Rothlisberger, U.; Nazeeruddin, M. K.; Grätzel, M. Dye-sensitized solar cells with 13% efficiency achieved through the molecular engineering of porphyrin sensitizers. *Nature Chemistry* **2014**, *6*, 242–247.
- (10) Huh, S.; Kim, S.-J.; Kim, Y. Porphyrinic metal–organic frameworks from custom-designed porphyrins. *CrystEngComm* **2016**, *18*, 345–368.
- (11) Fateeva, A.; Chater, P. A.; Ireland, C. P.; Tahir, A. A.; Khimyak, Y. Z.; Wiper, P. V.; Darwent, J. R.; Rosseinsky, M. J. A Water-Stable Porphyrin-Based Metal–Organic Framework Active for Visible-Light Photocatalysis. *Angewandte Chemie International Edition* **2012**, *51*, 7440–7444.
- (12) Kornienko, N.; Zhao, Y.; Kley, C. S.; Zhu, C.; Kim, D.; Lin, S.; Chang, C. J.; Yaghi, O. M.; Yang, P. Metal–Organic Frameworks for Electrocatalytic Reduction of Carbon Dioxide. *Journal of the American Chemical Society* **2015**, *137*, 14129–14135, PMID: 26509213.
- (13) Lions, M.; Tommasino, J.-B.; Chattot, R.; Abeykoon, B.; Guillou, N.; Devic, T.; Demessence, A.; Cardenas, L.; Maillard, F.; Fateeva, A. Insights into the mechanism of electrocatalysis of the oxygen reduction reaction by a porphyrinic metal organic framework. *Chem. Commun.* **2017**, *53*, 6496–6499.
- (14) Hamad, S.; Hernandez, N. C.; Aziz, A.; Ruiz-Salvador, A. R.; Calero, S.; Grau-Crespo, R. Electronic structure of porphyrin-based metal–organic frameworks and their suitability for solar fuel production photocatalysis. *J. Mater. Chem. A* **2015**, *3*, 23458–23465.

- (15) Aziz, A.; Ruiz-Salvador, A. R.; Hernández, N. C.; Calero, S.; Hamad, S.; Grau-Crespo, R. Porphyrin-based metal-organic frameworks for solar fuel synthesis photocatalysis: band gap tuning via iron substitutions. *J. Mater. Chem. A* **2017**, *5*, 11894–11904.
- (16) Ortega-Guerrero, A.; Fumanal, M.; Capano, G.; Tavernelli, I.; Smit, B. Insights into the Electronic Properties and Charge Transfer Mechanism of a Porphyrin Ruthenium-Based Metal–Organic Framework. *Chemistry of Materials* **2020**, *32*, 4194–4204.
- (17) Wu, X.-P.; Choudhuri, I.; Truhlar, D. G. Computational Studies of Photocatalysis with Metal–Organic Frameworks. *ENERGY & ENVIRONMENTAL MATERIALS* **2019**, *2*, 251–263.
- (18) Fumanal, M.; Capano, G.; Barthel, S.; Smit, B.; Tavernelli, I. Energy-based descriptors for photo-catalytically active metal–organic framework discovery. *J. Mater. Chem. A* **2020**, *8*, 4473–4482.
- (19) Kronik, L.; Stein, T.; Refaely-Abramson, S.; Baer, R. Excitation Gaps of Finite-Sized Systems from Optimally Tuned Range-Separated Hybrid Functionals. *Journal of Chemical Theory and Computation* **2012**, *8*, 1515–1531, PMID: 26593646.
- (20) Baerends, E. J. From the Kohn–Sham band gap to the fundamental gap in solids. An integer electron approach. *Phys. Chem. Chem. Phys.* **2017**, *19*, 15639–15656.
- (21) Bhandari, S.; Cheung, M. S.; Geva, E.; Kronik, L.; Dunietz, B. D. Fundamental Gaps of Condensed-Phase Organic Semiconductors from Single-Molecule Calculations using Polarization-Consistent Optimally Tuned Screened Range-Separated Hybrid Functionals. *Journal of Chemical Theory and Computation* **2018**, *14*, 6287–6294.
- (22) Izmaylov, A. F.; Scuseria, G. E. Why are time-dependent density functional theory excitations in solids equal to band structure energy gaps for semilocal functionals,



- and how does nonlocal Hartree–Fock-type exchange introduce excitonic effects? *The Journal of Chemical Physics* **2008**, *129*, 034101.
- (23) Refaely-Abramson, S.; Sharifzadeh, S.; Jain, M.; Baer, R.; Neaton, J. B.; Kronik, L. Gap renormalization of molecular crystals from density-functional theory. *Phys. Rev. B* **2013**, *88*, 081204.
- (24) Casida, M. E. In *Recent Advances in Density Functional Methods*; Chong, D. P., Ed.; 1995; pp 155–192.
- (25) Hirata, S.; Head-Gordon, M. Time-dependent density functional theory within the Tamm–Dancoff approximation. *Chemical Physics Letters* **1999**, *314*, 291 – 299.
- (26) Peach, M. J. G.; Tozer, D. J. Overcoming Low Orbital Overlap and Triplet Instability Problems in TDDFT. *The Journal of Physical Chemistry A* **2012**, *116*, 9783–9789, PMID: 22971224.
- (27) Perdew, J. P.; Burke, K.; Ernzerhof, M. Generalized Gradient Approximation Made Simple. *Phys. Rev. Lett.* **1996**, *77*, 3865–3868.
- (28) Perdew, J. P.; Ernzerhof, M.; Burke, K. Rationale for mixing exact exchange with density functional approximations. *The Journal of Chemical Physics* **1996**, *105*, 9982–9985.
- (29) Adamo, C.; Barone, V. Toward reliable density functional methods without adjustable parameters: The PBE0 model. *The Journal of Chemical Physics* **1999**, *110*, 6158–6170.
- (30) A new hybrid exchange–correlation functional using the Coulomb-attenuating method (CAM-B3LYP). *Chemical Physics Letters* **2004**, *393*, 51 – 57.
- (31) Frisch, M. J. *et al.* Gaussian~16 Revision C.01. 2016; Gaussian Inc. Wallingford CT.
- (32) Petersson, G. A.; Bennett, A.; Tensfeldt, T. G.; Al-Laham, M. A.; Shirley, W. A.; Mantzaris, J. A complete basis set model chemistry. I. The total energies of closed-shell

- atoms and hydrides of the first-row elements. *The Journal of Chemical Physics* **1988**, *89*, 2193–2218.
- (33) Pritchard, B. P.; Altarawy, D.; Didier, B.; Gibson, T. D.; Windus, T. L. New Basis Set Exchange: An Open, Up-to-Date Resource for the Molecular Sciences Community. *Journal of Chemical Information and Modeling* **2019**, *59*, 4814–4820, PMID: 31600445.
- (34) Hutter, J.; Iannuzzi, M.; Schiffmann, F.; VandeVondele, J. cp2k: atomistic simulations of condensed matter systems. *Wiley Interdisciplinary Reviews: Computational Molecular Science* **2014**, *4*, 15–25.
- (35) Kühne, T. D. *et al.* CP2K: An electronic structure and molecular dynamics software package - Quickstep: Efficient and accurate electronic structure calculations. *The Journal of Chemical Physics* **2020**, *152*, 194103.
- (36) Grimme, S.; Antony, J.; Ehrlich, S.; Krieg, H. A consistent and accurate ab initio parametrization of density functional dispersion correction (DFT-D) for the 94 elements H-Pu. *The Journal of Chemical Physics* **2010**, *132*, 154104.
- (37) Guidon, M.; Hutter, J.; VandeVondele, J. Robust Periodic Hartree-Fock Exchange for Large-Scale Simulations Using Gaussian Basis Sets. *Journal of Chemical Theory and Computation* **2009**, *5*, 3010–3021, PMID: 26609981.
- (38) Löwdin, P. On the Non-Orthogonality Problem Connected with the Use of Atomic Wave Functions in the Theory of Molecules and Crystals. *The Journal of Chemical Physics* **1950**, *18*, 365–375.
- (39) Goedecker, S.; Teter, M.; Hutter, J. Separable dual-space Gaussian pseudopotentials. *Phys. Rev. B* **1996**, *54*, 1703–1710.
- (40) VandeVondele, J.; Hutter, J. An efficient orbital transformation method for electronic structure calculations. *The Journal of Chemical Physics* **2003**, *118*, 4365–4369.

- (41) Guidon, M.; Hutter, J.; VandeVondele, J. Auxiliary Density Matrix Methods for Hartree-Fock Exchange Calculations. *Journal of Chemical Theory and Computation* **2010**, *6*, 2348–2364, PMID: 26613491.
- (42) Anderson, S. L.; Tiana, D.; Ireland, C. P.; Capano, G.; Fumanal, M.; Gładysiak, A.; Kampouri, S.; Rahmanudin, A.; Guijarro, N.; Sivula, K.; Stylianou, K. C.; Smit, B. Taking lanthanides out of isolation: tuning the optical properties of metal–organic frameworks. *Chem. Sci.* **2020**, *11*, 4164–4170.
- (43) Capano, G.; Ambrosio, F.; Kampouri, S.; Stylianou, K. C.; Pasquarello, A.; Smit, B. On the Electronic and Optical Properties of Metal–Organic Frameworks: Case Study of MIL-125 and MIL-125-NH<sub>2</sub>. *The Journal of Physical Chemistry C* **2020**, *124*, 4065–4072.
- (44) Hendrickx, K.; Vanpoucke, D. E. P.; Leus, K.; Lejaeghere, K.; Van Yperende Deyne, A.; Van Speybroeck, V.; Van Der Voort, P.; Hemelsoet, K. Understanding Intrinsic Light Absorption Properties of UiO-66 Frameworks: A Combined Theoretical and Experimental Study. *Inorganic Chemistry* **2015**, *54*, 10701–10710, PMID: 26540517.
- (45) TDDFT investigation on the solvent effect of methanol on the electronic structure and luminescence of metal organic framework CdL<sub>2</sub>. *Chemical Physics* **2019**, *523*, 70 – 74.
- (46) Wilbraham, L.; Coudert, F.-X.; Ciofini, I. Modelling photophysical properties of metal–organic frameworks: a density functional theory based approach. *Phys. Chem. Chem. Phys.* **2016**, *18*, 25176–25182.
- (47) Gouterman, M.; Wagnière, G. H.; Snyder, L. C. Spectra of porphyrins: Part II. Four orbital model. *Journal of Molecular Spectroscopy* **1963**, *11*, 108 – 127.
- (48) Lee, M. W.; Lee, D. L.; Yen, W. N.; Yeh, C. Y. Synthesis, Optical and Photovoltaic

- Properties of Porphyrin Dyes. *Journal of Macromolecular Science, Part A* **2009**, *46*, 730–737.
- (49) Zhang, A.; Kwan, L.; Stillman, M. J. The spectroscopic impact of interactions with the four Gouterman orbitals from peripheral decoration of porphyrins with simple electron withdrawing and donating groups. *Org. Biomol. Chem.* **2017**, *15*, 9081–9094.
- (50) Baerends, E.; Ricciardi, G.; Rosa, A.; van Gisbergen, S. A DFT/TDDFT interpretation of the ground and excited states of porphyrin and porphyrazine complexes. *Coordination Chemistry Reviews* **2002**, *230*, 5 – 27.
- (51) GmbH, P. L. 5,10,15,20-Tetrakis-(4-carboxyphenyl)-porphine-Zn(II). [https://porphyrin-laboratories.com/eng/catalog/Porphine-Base\\_Eng.php?Synonym=TCPP-Zn\(II\)&Name=5,10,15,20-Tetrakis-\(4-carboxyphenyl\)-porphine-Zn\(II\)&CAS=27647-84-3&Land=2&Index=11&Metall=30](https://porphyrin-laboratories.com/eng/catalog/Porphine-Base_Eng.php?Synonym=TCPP-Zn(II)&Name=5,10,15,20-Tetrakis-(4-carboxyphenyl)-porphine-Zn(II)&CAS=27647-84-3&Land=2&Index=11&Metall=30).
- (52) Sonkar, P. K.; Prakash, K.; Yadav, M.; Ganesan, V.; Sankar, M.; Gupta, R.; Yadav, D. K. Co(ii)-porphyrin-decorated carbon nanotubes as catalysts for oxygen reduction reactions: an approach for fuel cell improvement. *J. Mater. Chem. A* **2017**, *5*, 6263–6276.
- (53) Kümmel, S. Charge-Transfer Excitations: A Challenge for Time-Dependent Density Functional Theory That Has Been Met. *Advanced Energy Materials* **2017**, *7*, 1700440.
- (54) Chantzis, A.; Laurent, A. D.; Adamo, C.; Jacquemin, D. Is the Tamm-Dancoff Approximation Reliable for the Calculation of Absorption and Fluorescence Band Shapes? *Journal of Chemical Theory and Computation* **2013**, *9*, 4517–4525, PMID: 26589168.
- (55) Bertini, L.; Bruschi, M.; de Gioia, L.; Fantucci, P.; Greco, C.; Zampella, G. In *Atomistic Approaches in Modern Biology: From Quantum Chemistry to Molecular Simulations*; Reiher, M., Ed.; Springer Berlin Heidelberg: Berlin, Heidelberg, 2007; pp 1–46.

- (56) Casida, M.; Ipatov, A.; Cordova, F. In *Time-Dependent Density Functional Theory*; Marques, M. A., Ullrich, C. A., Nogueira, F., Rubio, A., Burke, K., Gross, E. K. U., Eds.; Springer Berlin Heidelberg: Berlin, Heidelberg, 2006; pp 243–257.
- (57) Hamad, S.; Hernandez, N. C.; Aziz, A.; Ruiz-Salvador, A. R.; Calero, S.; Grau-Crespo, R. Electronic structure of porphyrin-based metal–organic frameworks and their suitability for solar fuel production photocatalysis. *J. Mater. Chem. A* **2015**, *3*, 23458–23465.
- (58) Stassen, I.; Burtch, N.; Talin, A.; Falcaro, P.; Allendorf, M.; Ameloot, R. An updated roadmap for the integration of metal–organic frameworks with electronic devices and chemical sensors. *Chem. Soc. Rev.* **2017**, *46*, 3185–3241.
- (59) Egger, D. A.; Weissman, S.; Refaely-Abramson, S.; Sharifzadeh, S.; Dauth, M.; Baer, R.; Kümmel, S.; Neaton, J. B.; Zojer, E.; Kronik, L. Outer-valence Electron Spectra of Prototypical Aromatic Heterocycles from an Optimally Tuned Range-Separated Hybrid Functional. *Journal of Chemical Theory and Computation* **2014**, *10*, 1934–1952, PMID: 24839410.
- (60) Vrubel, I. I.; Senkevich, N. Y.; Khramenkova, E. V.; Polozkov, R. G.; Shelykh, I. A. Electronic Structure and Optical Response of Zn-Based Metal–Organic Frameworks. *Advanced Theory and Simulations* **2018**, *1*, 1800049.
- (61) Sun, H.; Ryno, S.; Zhong, C.; Ravva, M. K.; Sun, Z.; Körzdörfer, T.; Brédas, J.-L. Ionization Energies, Electron Affinities, and Polarization Energies of Organic Molecular Crystals: Quantitative Estimations from a Polarizable Continuum Model (PCM)-Tuned Range-Separated Density Functional Approach. *Journal of Chemical Theory and Computation* **2016**, *12*, 2906–2916, PMID: 27183355.
- (62) Xie, L. S.; Skorupskii, G.; Dincă, M. Electrically Conductive Metal–Organic Frameworks. *Chemical Reviews* **2020**, *0*, null, PMID: 32275412.

- (63) Wiktor, J.; Reshetnyak, I.; Ambrosio, F.; Pasquarello, A. Comprehensive modeling of the band gap and absorption spectrum of BiVO<sub>4</sub>. *Phys. Rev. Materials* **2017**, *1*, 022401.

## Graphical TOC Entry

Some journals require a graphical entry for the Table of Contents. This should be laid out “print ready” so that the sizing of the text is correct.

Inside the tocentry environment, the font used is Helvetica 8 pt, as required by *Journal of the American Chemical Society*.

The surrounding frame is 9 cm by 3.5 cm, which is the maximum permitted for *Journal of the American Chemical Society* graphical table of content entries.

The box will not resize if the content is too big: instead it will overflow the edge of the box.

This box and the associated title will always be printed on a separate page at the end of the document.